Solid–supercritical fluid phase equilibria

Benjamin C.-Y. Lu and Dingan Zhang

Department of Chemical Engineering, University of Ottawa, Ottawa,
Ontario, Canada, K1N 9B4

Abstract – Different types of phase behavior observed in binary mixtures
containing a solid and a supercritical fluid (SCF) are discussed at the
supercritical fluid extraction conditions. The pressure-temperature
(P-T) projection of the solid-liquid-gas (S-L-G) three-phase coexistence
curves together with the equilibrium liquid phase composition (x) values
were determined by the first freezing point (FFP) method. The equili-
brium cell was useful for the determination of liquid-gas critical loci
for the binary system, leading to the location of the upper critical
end point. The FFP technique was extended to ternary mixtures contain-
ing two solids. The PT projection of $solid_1$-$solid_2$-liquid-gas
(S_1-S_2-L-G) four-phase coexistence curves together with the x values of
the two solids were successfully determined. In addition, methods for
calculation of solid solubilities in SCF by means of cubic equations of
state are presented.

INTRODUCTION

Supercritical fluid extraction (SFE) is being developed as a practical separation process
for the food, flavor, pharmaceutical, chemical and energy industries. The application of
supercritical fluids (SCF) as extraction solvents is based on the observation of enhanced
solubility of solids and liquids in the solvents. The application of the SFE technology
often depends on our understanding of the phase behavior of mixtures in the critical
region. While phase diagrams for binary fluid mixtures are classified into six categories
and have been investigated in more detail (e.g. ref. 1-4), phase equilibria involving
solids at SFE conditions have not been so well studied. The concern here deals with phase
equilibria involving a SCF and one or two solids.

PHASE DIAGRAMS OF BINARY AND TERNARY MIXTURES

There are two types of solid-SCF phase diagrams for binary mixtures. The triple point
temperature of the solid under consideration is greater than the critical temperature of
the SCF. There is no common range of temperature in which both pure components are in the
liquid state. The simplest pressure-temperature (P-T) projection curve (Type I) is that
for a mixture with the critical mixture curve runs continuously between the critical points
of the two components. A continuous three-phase solid-liquid-gas (S-L-G) curve is
observed. The phase behavior of the systems sodium chloride-water (ref. 5) and carbon
dioxide-methane (ref. 6) follows Type I. Binary mixtures of Type I are of little interest
to SFE operations. In this discussion emphasis is placed on the second class (Type II) of
mixtures, in which the critical-mixture and the S-L-G curves are not continuous. Type II
usually occurs for mixtures whose components are not chemically similar and differ consi-
derably in size, shape and polarity. The lower-temperature branch of the SLG curve inter-
sects the critical mixture curve at the lower critical end point (LCEP). The solubility of
the solid in the vapor (or gas) phase increases very rapidly at the LCEP. However, the
amount of solid in the SCF phase is rather low. The higher-temperature branch of the S-L-G
curve begins at the triple point temperature of the solid and ends at the upper critical
end point (UCEP), the intersection of the critical mixture curve and the S-L-G curve. The
solid solubility is an extremely strong function of temperature and pressure in the UCEP
region, at temperatures slightly below the UCEP temperature and in the vicinity of the UCEP
pressure. Phase diagrams for Type II mixtures may be further classified into three catego-
ries according to the shape of the higher-temperature branch of the S-L-G curve:

Type IIa: The S-L-G curve has a negative slope. The phase behavior of the mixtures con-
taining ethylene such as naphthalene-ethylene (ref. 7) and biphenyl-ethylene (ref. 8)
belongs to this group.

Type IIb: The S-L-G curve has a temperature minimum below the triple point temperature of
the solid and the UCEP temperature. The phase behavior of the mixtures containing carbon
dioxide such as naphthalene-carbon dioxide and biphenyl - carbon dioxide (ref. 9-11)
belongs to this group.
Type IIc: The S-L-G curve has a positive slope. The phase behavior of hydrogen-carbon
dioxide (ref. 12) and neon-argon (ref. 13) at cryogenic conditions belongs to this group.

The pressure-temperature-composition (P-T-x) diagram as well as the pressure-temperature
and pressure-composition projections of the P-T-x diagram of Type I and the three sub-
groups of Type II are represented schematically in Fig. 1.

Experimental investigation of phase equilibria for ternary mixtures consisting a SCF and
two nonvolatile solids is rather limited in spite of their practical usefulness.
Koningsveld and Diepen (ref. 14) suggested that three main types of such ternary mixtures
can be distinguished according to the extent of the existence of binary and ternary criti-
cal end points:

Type I: Systems without ternary critical end points (TCEP), but with binary critical end
points (BCEP) of the SCF and one of the solids.
Type II: Systems without TCEP but with BCEP formed from the SCF with both of the solids.
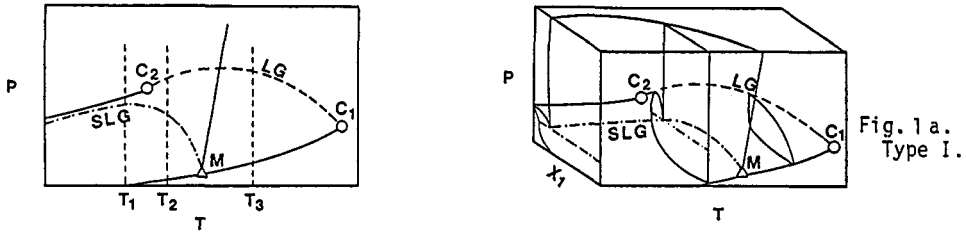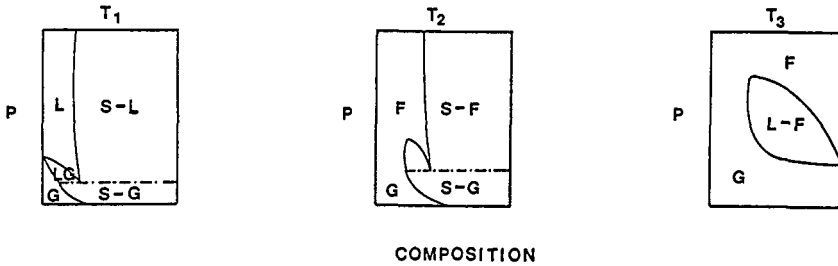Type III: Systems with BCEP and TCEP.

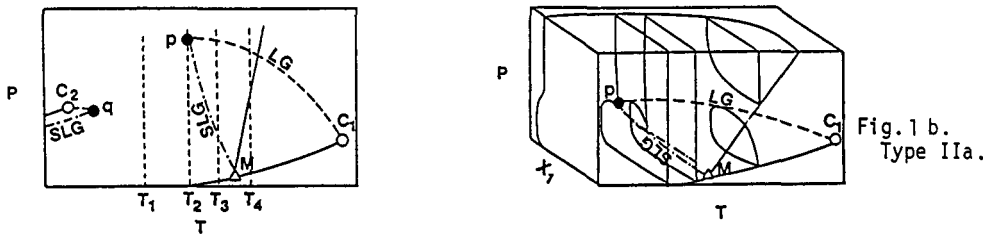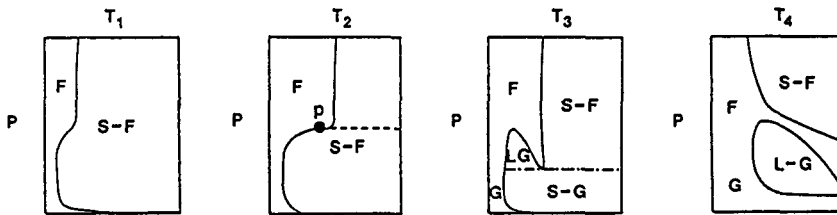
Fig. 1 a.
Type I.

COMPOSITION
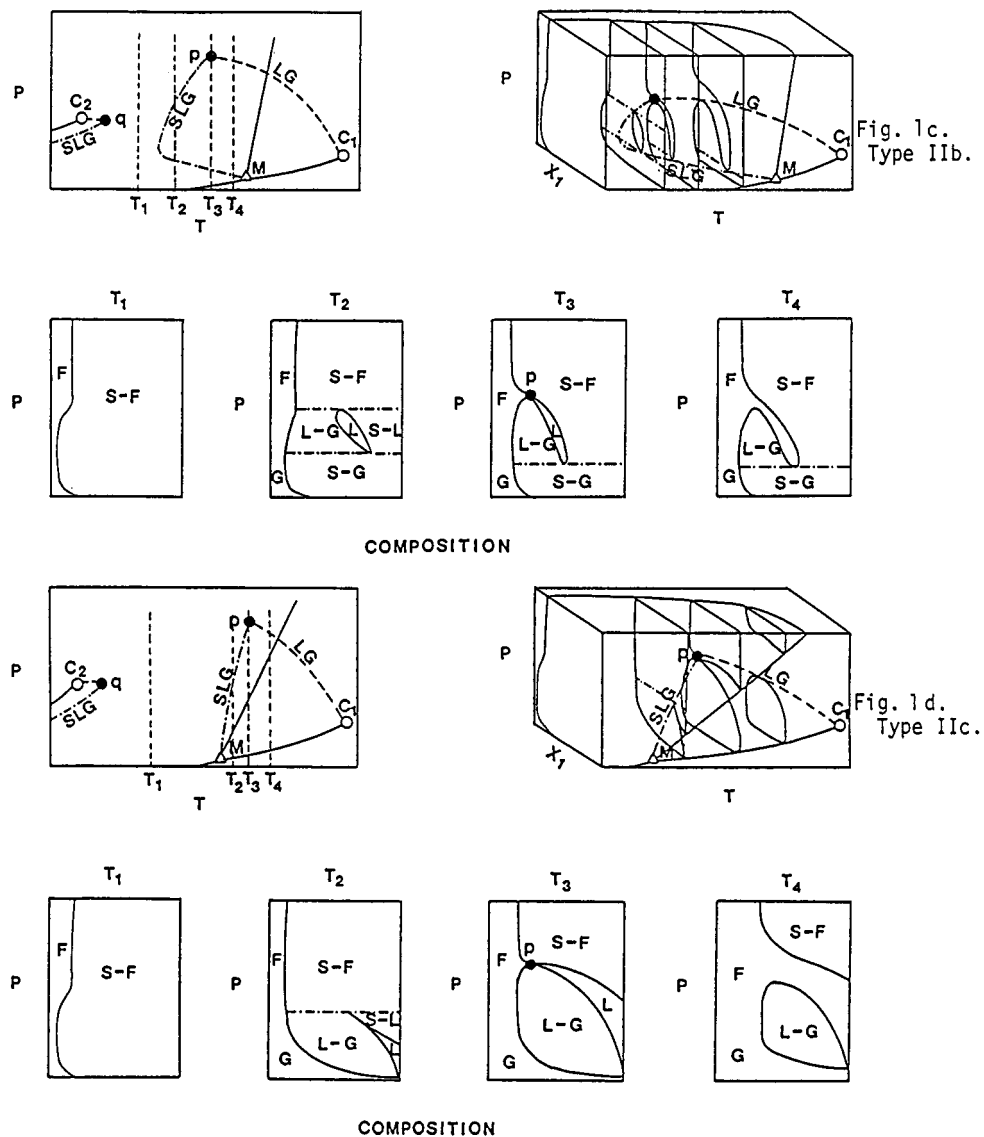

Fig. 1 b.
Type IIa.

COMPOSITION

Fig. 1. Pressure-temperature-composition diagram and pressure-temperature and pressure-composition projections for binary mixtures with a supercritical fluid and a slightly volatile component. -----, L = G loci; —·—·—·, three-phase S-L-G coexistence curve; C_1, C_2, critical points; M, triple point; p, upper critical end point; q, lower critical end point.

The phase behavior of Type III represents the most probable situation if the solubilities of both of the solids in the SCF are small (ref. 14, 15). For temperatures between the ternary LCEP and UCEP there are two solids in equilibrium with a fluid phase at any pressure. The two S_1-S_2-L-G four-phase coexistence curves, one ends with the ternary LCEP and the other with the ternary UCEP, form the boundaries for SFC operations. It should be mentioned that S_1-S_2-L-G curves reported in the literature are limited to very few systems (ref. 16, 17).

FIRST FREEZING POINT METHOD FOR MULTIPHASE COEXISTENCE CURVE AND EQUILIBRIUM LIQUID COMPOSITION DETERMINATIONS

There is no lack of experimental effects in the determination of solubilities of solids in SCF with or without a co-solvent (entrainer). However, the experimental results on the multiphase coexistence curves (S-L-G for binary and S_1-S_2-L-G for ternary mixtures) are rather limited. Different techniques are described in the literature for determination of these multiphase coexistent curves. Van Welie and Diepen (ref. 18) made P-T measurements at various constant compositions. The intersections of the liquid-gas and the solid-gas

isopleths yield the P-T projection of the three-phase curve. In another approach (ref. 7, 9, 10), the P-T projection of the three-phase curve was determined by slowly increasing the temperature of an initial solid-gas condition at constant pressure until the solid begins to melt, and the temperature was taken to be the three-phase temperature. This is the so-called "first melting point" (FMP) method. In the approach of van Welie and Diepen (ref. 18), composition of both the liquid and the vapor phases along the three-phase curve were determined, but the procedure is tedious and time consuming. The FMP method is relatively straightforward. However, it would be difficult to determine the liquid phase composition. The uniformity of the liquid phase composition could not be ensured, because difficulties encountered in agitating the cell content at the first melting of the solid.

In an effort to improve the performance of the FMP method, a technique was developed in our laboratory for determination of the P-T projection of the S-L-G curve by observing the initial appearance of the solid phase. This technique was named as the "first freezing point" (FFP) method. The initial temperature of a liquid-gas condition was decreased slowly at constant pressure until the first appearance of the solid phase could be observed. It is preferred to start from the low pressure end for the determination of the coexistence curve. The results obtained for the systems naphthalene-carbon dioxide and biphenyl-carbon dioxide (ref. 11) were found to be more self consistent than the results obtained from the FMP method. Provisions were made with the apparatus for taking liquid samples at the three-phase condition. A schematic diagram is shown in Figure 2. Details of the operation procedure have been reported elsewhere (ref. 16). The P-T projection of S-L-G curves for four binary mixtures containing naphthalene, biphenyl, m-terphenyl and phenanthrene with the supercritical carbon dioxide is shown in Figure 3. The phase behavior of all of these four systems follows Type IIb of Fig. 1, as a temperature minimum occurs in the P-T projection. The FFP method has been extended to the determination of the four-phase (S_1-S_2-L-G) coexistence curves for two ternary systems consisting of carbon dioxide and two solids (ref. 16).
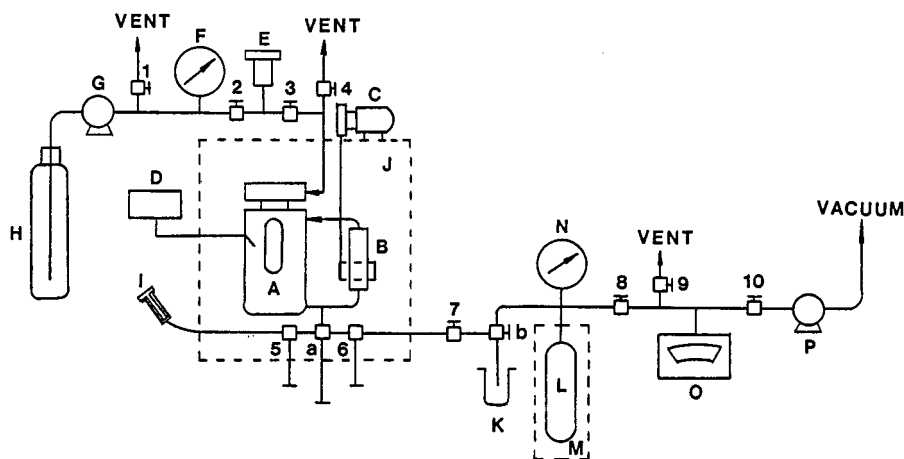

Fig. 2. Schematic diagram of apparatus. A- Dual window equilibrium cell; B- Magnetic pump; C- Variable-speed motor; D- Temperature indicator; E- Pressure transducer; F- Pressure gauge; G- Pressure intensifier; H- Liquid carbon dioxide cylinder; I- Syringe; J- Air bath; K- Solid sampler; L- Sample cylinder; M- Water bath; N- Pressure gauge; O- Thermocouple gauge; P- Vacuum pump; a, b - Three way valves; 1 to 10 - Valves.

For systems containing a SCF and a slightly volatile solid, very few systems have been investigated as far as the equilibrium liquid phase compositions along the three-phase coexistence curves are concerned. Other than the values reported by van Welie and Diepen (ref. 18, 19) for the systems naphthalene-ethylene and naphthalene-ethane, it appears that only data reported in the literature are those from our laboratory (ref. 11, 16) for the binary systems naphthalene-carbon dioxide, biphenyl-carbon dioxide and phenanthrene-carbon dioxide; and the ternary systems naphthalene-biphenyl-carbon dioxide and naphthalene-phenanthrene-carbon dioxide. The P-T-x values along the S-L-G curve for the binary system m-terphenyl-carbon dioxide are presented in Table 1 to serve as an example.

The liquid composition values along multiphase coexistence curves are useful for studying of phase diagrams and for testing and developing thermodynamic models for data representation, reduction and prediction. They are useful in the study of the relationship between the solubility of the SCF in the equilibrium liquid and the melting-point depression curve
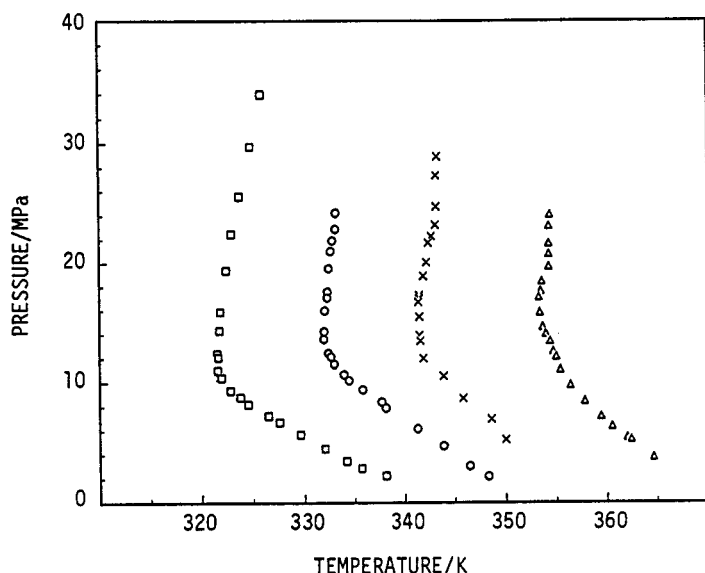
Fig. 3. Pressure-temperature
projection of three-phase
(S-L-G) coexistence curves
for four binary mixtures

O Naphthalene-carbon dioxide
□ Biphenyl - carbon dioxide
X m-Terphenyl-carbon dioxide
△ Phenanthrene-carbon dioxide

TABLE 1. P-T-x data of the three-phase coexistence curve for m-terphenyl(1)-CO_2(2).

P/MPa	T/K	x_1	P/MPa	T/K	x_1
5.25	350.0	0.771	17.30	341.4	0.536
6.97	348.6	-	18.91	341.8	0.528
8.70	345.8	0.688	20.08	342.1	0.517
10.56	343.9	0.676	21.74	342.4	0.504
12.02	341.9	0.621	22.31	342.7	-
13.49	341.5	0.602	23.24	343.1	0.516
13.96	341.4	0.582	24.77	343.2	0.502
15.48	341.4	0.544	27.32	343.2	0.513
16.72	341.3	-	28.90	343.3	0.506
17.03	341.4	-			

(ref. 20). The P-T projection curves shown in Fig. 3 together with the liquid compositions
of carbon dioxide x_2 for these systems (Table 1 and ref. 11, 16) verify that the freezing-
point depressions at the triple point of the solid are greater the higher the x_2 values.

DETERMINATION OF UCEP

The upper critical end point UCEP may be considered as a limit case in which the liquid-gas
equilibrium (L = G) becomes identical with the S-L-G equilibrium. It is the intersection
of the L = G loci and the S-L-G curves on the P-T projection. The location of UCEP plays
an important role in the selection of operating conditions for SFE processes. The impor-
tance of knowing the UCEP location may be illustrated using the solubility of naphthalene
in supercritical ethylene. The UCEP for this system was experimentally determined by van
Gunst et al. (ref. 7) to be at 325.2 K and 17.64 MPa, using the intersection technique.
The solubility data reported by Diepen and Scheffer (ref. 21) for the same system indicated
that the isotherm of 323.2 K has a slight slope [i.e. $(\partial P/\partial y)_T$ is small] in the vicinity
of 17 to 18 MPa. In other words, the solubility enhancement of naphthalene in supercri-
tical ethylene is very sensitive to a small change of pressure in the vicinity of the UCEP
pressure. At the UCEP pressure, $(\partial P/\partial y)_T = 0$. Similar observation was obtained with the
variation of temperature. Namely, $(\partial T/\partial y)_p$ is small in the vicinity of the UCEP tempera-
ture and $(\partial T/\partial y)_p = 0$ at the UCEP temperature. It is this sensitity of the solubility with
small changes in pressure or temperature in the vicinity of the UCEP that provides the
opportunity for SFE processes.

In addition to the intersection method, McHugh and Paulaitis (ref. 22) estimated the UCEP
for naphthalene and biphenyl in supercritical carbon dioxide based on the characteristics
of the P-y curves, and McHugh and Yogan (ref. 10) determined the UCEP for several binary
system by observing the pressure and temperature at which critical opalescence is observed
along the S-L-G curve for a very slight change in either pressure or temperature.

The apparatus used in the FFP method as shown in Fig. 2 was used in our laboratory for

determination of the L = G critical loci for the naphthalene-carbon dioxide system. In the
determination, bubble point pressure along the isotherms of 338.2, 343.2 and 348.2 K as
well as the solubility of carbon dioxide in liquid naphthalene were measured. A brief
description of the procedure is given here. The equilibrium cell A was purged with carbon
dioxide before solid naphthalene was changed. The temperature of the air bath was raised
until the solid in the cell was melted completely. Then the cell was purged again with
carbon dioxide. The temperature of the air bath could be adjusted to the desired tempera-
ture ± 0.05 K. The temperature of the cell was monitored by two thermocouples. Liquid
carbon dioxide was compressed by the pressure intensifier G, introduced to and vaporized in
the cell until the pressure in the cell was brought to an appropriate level. The accuracy
of the pressure measurement was estimated to be ± 0.05 MPa. The liquid mixture in the cell
was recirculated by means of the magnetic pump B. The equilibrium condition was reached
when there was no more change of the system pressure at the desired temperature. Sampling
of the liquid phase was made 30 to 40 min. after the equilibrium pressure was reached. The
accuracy of the liquid composition determination is estimated to be ± 0.005 mole fraction.
For each isotherm, the experiments were carried out until the liquid-gas critical point was
reached. At the critical point, the meniscus between the liquid and gas phases disap-
peared, the mixture in the cell turned scarlet and the critical opalescence reached its
maximum intensity. When pressure of the system was further increased above the critical
point, the scarlet color disappeared and only one phase existed in the cell.

TABLE 2.   Solubility of carbon dioxide (2) in naphthalene (1).

T/K	x_2	P/MPa	x_2	P/MPa	x_2	P/MPa
348.2	0.09	2.23*	0.495	12.66	0.708	24.17
	0.185	4.12	0.535	14.08	0.711	24.25
	0.245	5.77	0.574	15.95	0.726	24.99
	0.299	7.39	0.576	16.00	0.741	25.46
	0.359	8.86	0.605	18.01	0.754	25.96
	0.424	10.41	0.635	20.05	0.787	26.26 (C.P.)
	0.425	10.46	0.667	22.11		
343.2	0.20	5.07*	0.571	13.51	0.708	22.55
	0.311	6.43	0.609	15.58	0.733	24.26
	0.312	6.46	0.638	17.62	0.773	25.74
	0.411	8.99	0.657	19.39	0.804	26.20 (C.P.)
	0.507	11.28	0.658	19.44		
338.2	0.32	7.90*	0.630	14.50	0.745	22.40
	0.483	10.12	0.666	16.18	0.763	24.01
	0.544	11.48	0.700	18.45	0.781	25.30
	0.590	12.94	0.711	20.06	0.822	26.10 (C.P.)

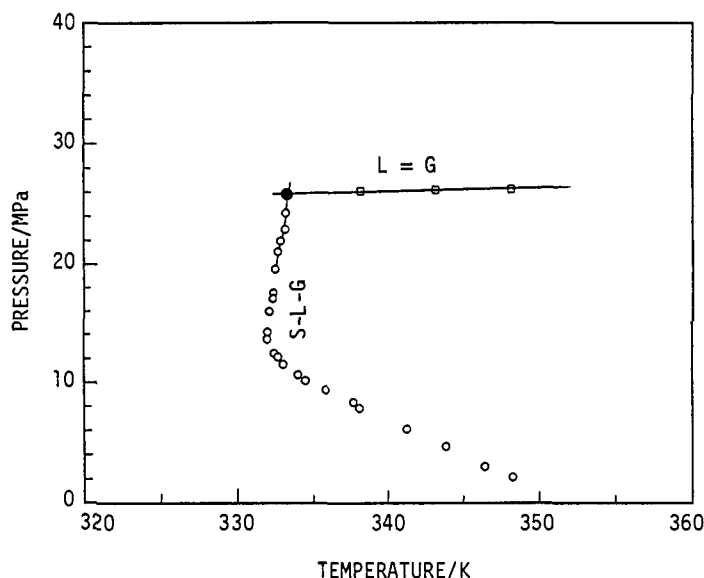* Interpolated from the S-L-G curve of the system (ref. 11)

Fig. 4. Determination of the
upper-critical-end-point for
the naphthalene-carbon dioxide
system by means of the inter-
section method.

The experimentally determined P-T-x values at the three temperatures for the naphthalene-carbon dioxide system are reported in Table 2. The P-T projections of the L = G critical loci and the S-L-G curve are presented in Fig. 4. The temperature and pressure of the UCEP for naphthalene-carbon dioxide were established to be 333.4 K and 25.9 MPa, respectively. The corresponding values reported in the literature are 336.2 K and 24.3 MPa (ref. 22), and 333.3 K and 25.6 MPa (ref. 10). Although the values obtained from the intersection method are more reliable, the estimated values obtained from the other two approaches appear to be close enough for engineering approximations.

CALCULATION OF SOLID SOLUBILITIES IN SCF BY MEANS OF CUBIC EOS

The application of analytical expressions, such as an equation of state (EOS), to the representation of pressure-temperature-composition along the multiphase coexistence curves requires further studies. On the other hand, some improvements on the representation of solid solubilities have been achieved.

Solubility data at high pressures are needed to evaluate and design separation processes using supercritical fluids. Dynamic or flow methods, either single-pass or vapor-recirculation, and static methods have been used for determination of solubility of solids in SCF. It is desirable to minimize the experimental effort by methods of correlation and prediction. An expression directly relating the concentration of solute to the density of the extraction fluid or an EOS may be used to represent and estimate solubility data at SFE conditions. The relationship between the concentration of a solute in a compressed gas, c, and the gas density d proposed by Stahl et al. (ref. 23),

$$\ln c = m \ln d + \text{constant} \tag{1}$$

may serve as an example for the first approach. Recently, a five-parameter cubic EOS of the van der Waals type (ref. 24)

$$P = \frac{RT}{(V-b)} - \frac{a(V-c)}{(V-b)(V-d)(V+e)} \tag{2}$$

was developed specifically for representing pure-component volumetric properties. The parameters were generalized in terms of critical temperature T_c and the acentric factor ω. In addition, individual parameters for carbon dioxide, ethylene, ethane and propane were presented for predicting volumetric behaviors in the critical region useful for calculating the quantity d of eqn. (1).

Many equations of state have been applied to the calculation of supercritical solubilities. Adachi and Lu (ref. 25) used the Redlich-Kwong (RK) equation as modified by Soave (SRK) (ref. 26), the Peng-Robinson (PR) equation (ref. 27) and the four-parameter equation proposed by Adachi et al. (ref. 28) for representing the binary solubility data for a number of solutes in supercritical carbon dioxide and ethylene. The solubilities of naphthalene and benzoic acid in these two gases were found to be satisfactorily represented by any one of these equation, but the solubilities of phenanthrene and anthracene in these two gases were not. Haselow et al. (ref. 29) evaluated eight cubic EOS and an eleven-parameter equation of the BWR type and concluded that these equations together with the classical one fluid mixing rules were not adequate for quantitative representation of supercritical solubility.

The solubility of a solid (1) in a compressed gas (2) may be expressed by

$$y_1 = P_1^S \exp [\tilde{V}_1^S(P - p_1^S)/RT]/P\phi_1 \tag{3}$$

with the assumptions that (i) the solubility of the gas in the solid is negligible and (ii) the solid volume remains practically constant. In eqn. (3), $\tilde{V}_1^S$ is the molar volume of the solid, p_1^S is the vapor pressure of the solid and ϕ_1 is the fugacity coefficient of the solid in the gas phase. The quantity ϕ_1 is given by

$$RT\ln\phi_1 = \int_V^\infty [(\partial P/\partial n_1)_{T,V,n_2} - RT/V]dV - RT \ln Z \tag{4}$$

and can be calculated by means of an EOS.

In an effort to determine the controlling variable in the evaluation of the key quantity ϕ_1, Adachi et al. (ref. 30) recently considered the VDW type cubic EOS of the form

$$P = RT/(V-b_1) - a/(V-b_2)(V-b_3) \tag{5}$$

with $b_2 \neq b_3$. Many simple cubic EOS can be represented by eqn. (5). The VDW equation is obtained by letting $b_2 = b_3 = 0$; the Clausius equation, $b_2 = b_3 = c$; the RK (or the SRK) equation, $b_2 = 0$ and $b_3 = b_1$; and the PR equation, $b_2 = b_1(-1 + 2^{\frac{1}{2}})$ and $b_3 = b_1(-1 - 2^{\frac{1}{2}})$. In eqn. (5)

$$a = \Omega_a R^2 T_c^2 / P_c \tag{6}$$

$$b_k = \Omega_{bk} RT_c / P_c, \quad k = 1, 2, 3 \tag{7}$$

Using the conventional mixing rules for a and b_k

$$a = \Sigma\Sigma y_i y_j a_{ij}, \quad a_{ij} = (a_i a_j)^{\frac{1}{2}} (1 - k_{ij}) \tag{8}$$

$$b_k = \Sigma y_i b_{ki}, \quad k = 1, 2, 3 \tag{9}$$

The expression for $\ln\phi_1$ is obtained as follows:

$$\ln\phi_1 = \ln[RT/P(V-b_1)] + b_{11}/(V-b_1) + [2\Sigma y_j a_{1j}/RT(b_2-b_3)] \ln[(V-b_2)/(V-b_3)]$$

$$- [a/RT(b_2-b_3)] [b_{21}/(V-b_2) - b_{31}/(V-b_3)]$$

$$- \{[a(b_{21}-b_{31})]/[RT(b_2-b_3)^2]\} \ln[(V-b_2)/(V-b_3)] \tag{10}$$

The characteristics of the quantities involved in eqn. (10) based on an earlier study (ref. 31) are:

1. The mixture terms (b_2-b_3), $(V-b_1)$, $(V-b_2)$ and $(V-b_3)$ are functions of the parameters "a" of the mixture, a_{mix}.
2. The quantities b_{21} and b_{31} (the pure-component parameters b_2 and b_3 for the solid) are functions of Ω_{a1} and b_{11}. Their values are fixed when Ω_{a1} and b_{11} are specified.
3. The parameter b_k of the SCF (b_{12}, b_{22} and b_{32}) do not play a role in the calculation of ϕ_1.

Consequently, ϕ_1 of eqn. (10) is controlled by a_{mix} and b_{11}. In other words, it is controlled by Ω_a of both of the components, k_{ij} of eqn. (8) and the covolume of the solid b_{11} (or Ω_{b11}). The effect of Ω_{b11} on the solubility of fluorence in carbon dioxide using the
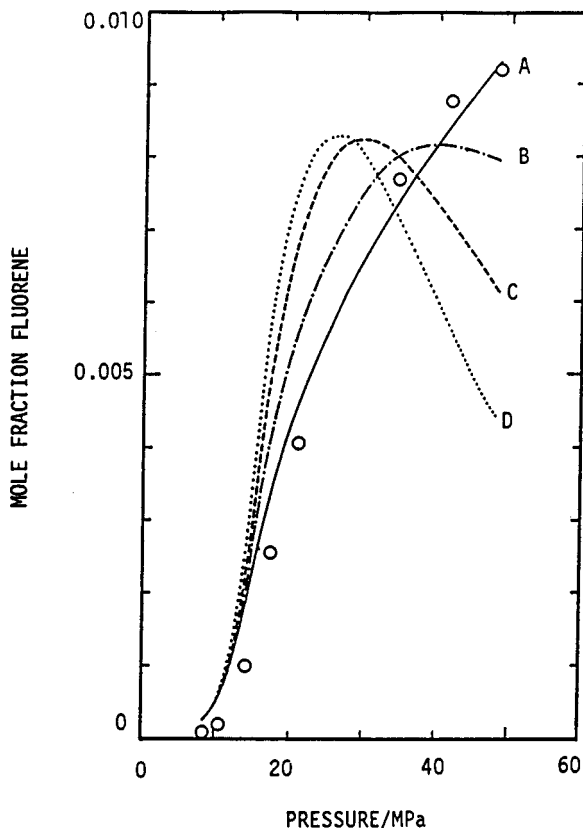

Fig. 5. Representation of solubility of fluorene in carbon dioxide at 343.15 K (ref. 32) using the Peng-Robinson equation. Curve A: Ω_{b11} = 0.0405, k_{12} = 0.222; Curve B: Ω_{b11} = 0.0574, k_{12} = 0.193; Curve C (original PR): Ω_{b11} = 0.0778, k_{12} = 0.162; Curve D: Ω_{b11} = 0.0984, k_{12} = 0.136.

PR equation is illustrated in Fig. 5. A better representation was achieved with a judi-
cially selected value of b_{11}.

Yamamoto et al. (ref. 33) pointed out that mixing rules are more important than the selec-
tion of EOS. Adachi et al. (ref. 30) replaced the mole fraction terms of eqns. (6) and (7)
by means of a "characteristic fraction" θ,

$$\theta_i = x_i\gamma_i/\Sigma x_i\gamma_i \tag{11}$$

where γ is the characteristic parameter of component i. Hence,

$$a = \Sigma\Sigma\theta_i\theta_ja_{ij}, \quad a_{ij} = (a_ia_j)^{\frac{1}{2}} (1 - k_{ij}) \tag{12}$$

$$b_k = \Sigma\theta_ib_{ki}, \quad k = 1, 2, 3 \tag{13}$$

and $\ln\phi_1$ is given by

$$\ln\phi_1 = \ln[RT/P(V-b_1)] + [b_1 + (b_{11} - b_1) \gamma_1/\Sigma x_i\gamma_i]/(V-b_1)$$

$$+ \{[a(1 + \gamma_1/\Sigma x_i\gamma_i) + n(\partial a/\partial n_1)]/[RT(b_2-b_3)] -$$

$$[a(b_{21}-b_{31}) \gamma_1/\Sigma x_i\gamma_i]/[RT(b_2-b_3)^2]\}\cdot\ln[(V-b_2)/(V-b_3)]$$

$$- a/[RT(b_2-b_3)] \{[b_2 + (b_{21}-b_2)\gamma_1/\Sigma x_i\gamma_i]/(V-b_2)$$

$$- [b_3 + (b_{31}-b_3) \gamma_1/\Sigma x_i\gamma_i]/(V-b_3)\} \tag{14}$$

In which $n = \Sigma n_i$ and $x_i = n_i/n$. The difference between the calculated values obtained from
the "characteristic fraction" approach and those obtained from the "mole fraction" approach
on the solubility of phenanthrene in carbon dioxide using the PR equation is shown in Fig.
6. The new approach reduces the deviations and yields a correct trend for the variation of
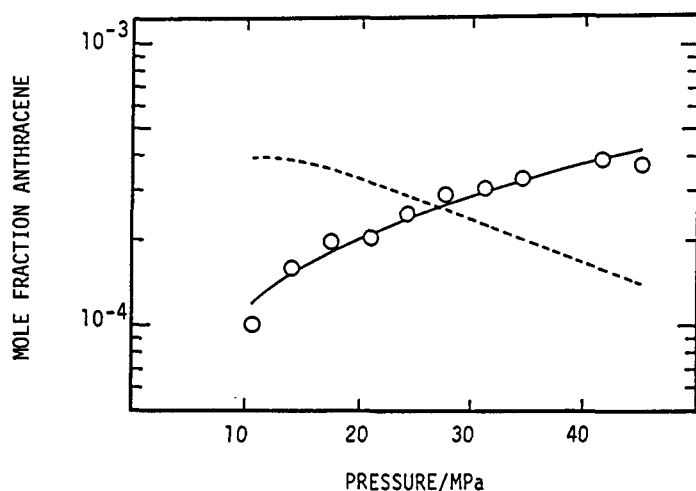y_1 with pressure.

Fig. 6. Comparison of calculated
solubility of anthracene in
ethane at 323.15 K (ref. 32)
using the Peng-Robinson
equation. —— characteristic
fraction, ---- mole fraction.

The calculated results (ref. 30) indicate that by treating $\Omega_{b_{11}}$ as a variable or by replac-
ing mole fractions with characteristic fractions improve the ability of simple cubic EOS to
describe solid solubilities in SCF, but the selection of EOS is not crucial.

CONCLUDING REMARKS

The available data indicate that there is a temperature minimum on the multiphase coexis-
tence curve for the binary and ternary systems with carbon dioxide as the supercritical
fluid and naphthalene, biphenyl, m-terphenyl, phenanthrene and octacosane as the slightly
volatile component(s); and that there is no temperature minimum on the multiphase coexis-
tence curve for the binary and ternary systems with ethylene as the supercritical fluid and
*naphthalene, biphenyl, hexachloroethane and octacosane as the slightly volatile compo-
nent(s).

The first freezing point appears to be suitable for the determination of multiphase coexistence curves for binary and ternary system leading to the upper critical end point.

The representation of solubility data by adjusting the parameter b_1 for the solid or by applying an empirical "characteristic fraction" seems to be promising.

Acknowledgement

REFERENCES

1. P.H. van Konynenburg and R.L. Scott, Phil. Trans. Roy. Soc., London, A298 495-540 (1980).
2. G.M. Schneider, in Chemical Thermodynamics Vol 2, M.L. McGlashan, ed., A Specialist Periodical Report, The Chemical Society, London, 1978, Chap. 4, pp. 105-146.
3. M.L. McGlashan, Pure Appl. Chem., 57, 89-103 (1985).
4. C.L. Young, in Chemical Thermodynamics Vol 2, M.L. McGlashan, ed., A Specialist Periodical Report, The Chemical Society, London, 1978, Chap. 3, pp. 71-104, Pure Appl. Chem., 58, 1561-1572 (1986).
5. J.S. Rowlinson and M.J. Richardson, Adv. Chem. Phys., 2, 85-118 (1959).
6. H.G. Donnelly and D.L. Katz, Ind. Eng. Chem., 46, 511-517 (1954).
7. C.A. van Gunst, F.E.C. Scheffer and G.A.M. Diepen, J. Phys. Chem., 57, 578-581 (1953).
8. G.A.M. Diepen and F.E.C. Scheffer, J. Am. Chem. Soc., 70, 4081-4085 (1948).
9. A. Prins, Proc. Roy. Acad. Amsterdam, 17, 1090-1111 (1915).
10. M.A. McHugh and T.J. Yogan, J. Chem. Eng. Data, 29, 112-115 (1984).
11. P.L. Cheong, D. Zhang, K. Ohgaki and B.C.-Y. Lu, Fluid Phase Equilibria, 29, 555-562 (1986).
12. C.Y. Tsang and W.B. Streett, Chem. Eng. Sci., 36, 993-1000 (1981).
13. W.B. Streett and J.L.E. Hill, J. Chem. Phys., 54, 5088-5094 (1971).
14. R. Koningsveld and G.A.M. Diepen, Fluid Phase Equilibria, 10, 159-172 (1983).
15. R. Koningsveld, L.A. Kleintjens and G.A.M. Diepen, Ber. Bunsenges. Phys. Chem., 88, 848-855 (1984).
16. D. Zhang, Y. Adachi and B.C.-Y. Lu, Proc. Inter. Sym. Supercritical Fluids, Nice, France in press (1988).
17. C.A. van Gunst, F.E.C. Scheffer and G.A.M. Diepen, J. Phys. Chem., 57, 581-583 (1953).
18. G.S.A. van Welie and G.A.M. Diepen, Rec. trav. chim., 80, 659-680 (1961).
19. G.S.A. van Welie and G.A.M. Diepen, J. Phys. Chem., 67, 755-757 (1963).
20. J. de Swaan Arons and G.A.M. Diepen, Rec. trav. chim., 82, 249-256 (1963).
21. G.A.M. Diepen and F.E.C. Scheffer, J. Phys. Chem., 57, 575-577 (1953).
22. M.A. McHugh and M.E. Paulaitis, J. Chem. Eng. Data, 25, 326-329 (1980).
23. E. Stahl, W. Schilz, E. Schültz and Willing, Angew. Chem. Int. Ed. Engl., 17, 731-738 (1978).
24. Y. Adachi, H. Sugie and B.C.-Y. Lu, Fluid Phase Equilibria, 28, 119-136 (1986).
25. Y. Adachi and B.C.-Y. Lu, Fluid Phase Equilibria, 14, 147-156 (1983).
26. G. Soave, Chem. Eng. Sci., 27, 1197-1203 (1972).
27. D.Y. Peng and D.B. Robinson, Ind. Eng. Chem. Fundam., 15, 59-64 (1976).
28. Y. Adachi, B.C.-Y. Lu and H. Sugie, Fluid Phase Equilibria, 11, 29-48 (1983).
29. J.S. Haselow, S.J. Han, R.A. Greenkorn and K.C. Chao, ACS Symp. Ser. 300, 156-178 (1986).
30. Y. Adachi, H. Sugie and B.C.-Y. Lu, Proc. Inter. Sym. Thermodyn. Chem. Eng. Ind., Beijing, China, 218-229 (1988).
31. Y. Adachi and B.C.-Y. Lu, Can. J. Chem. Eng., 63, 497-503 (1985).
32. K.P. Johnston, D.H. Ziger and C.A. Eckert, Ind. Eng. Chem. Fundam., 21, 191-197 (1982).
33. H. Yamamota, Y. Iwai, Y. Arai and B.C.-Y. Lu, Proc. Inter. Sym. Thermodyn. Chem. Eng. Ind., Beijing, China, 456-463 (1988).